Dissolution Modeling: Factors Affecting the Dissolution Rates of Polydisperse Powders

Allan T. K. Lu,[1] Mary E. Frisella,[1] and Kevin C. Johnson[1,2]

Received October 7, 1992; accepted March 2, 1993

The dissolution rates of two lots of hydrocortisone (fine and coarse) were simulated using a computer program based on a Noyes–Whitney-type equation. Derivations of the equation were made to compare the accuracy of simulations using spherical and cylindrical particle geometry, with and without a time-dependent diffusion layer thickness. To approximate better the shape of the hydrocortisone particles, a shape factor was used to relate cylindrical length to radius. The most accurate simulations were obtained by assuming cylindrical geometry with and without a time-dependent diffusion layer thickness for the fine and coarse hydrocortisone, respectively. The program was also modified to simulate initial particle size distributions based on the log normal probability density function.

KEY WORDS: computer simulation; dissolution modeling; particle shape; diffusion layer thickness; log normal distribution; hydrocortisone.

INTRODUCTION

Methods for predicting the effect of dissolution rate on oral absorption have been previously reported (1,2). Using a Noyes–Whitney-type equation (3) derived for spherical particles, these methods can be used to simulate dissolution under nonsink conditions if the solubility and particle size of the drug are known, and if assumptions are made regarding the hydrodynamics of the system.

To explore the effect of model assumptions, we have refined a computer program (2) by including a time-dependent diffusion layer thickness or nonspherical geometry in an attempt to improve the accuracy of simulated dissolution rates. The dissolution rates of two lots of hydrocortisone served to gauge the extent of improvement from the alterations.

Standard methods for characterizing polydisperse powders based on log-normal distributions (4–10) were also adopted and incorporated into the computer program so that dissolution rates could be simulated using geometric means and standard deviations of particle size distributions. This improved the efficiency in simulating dissolution rates as well as specifying the particle size distributions used in the simulations.

MATERIALS AND METHODS

Hydrocortisone Samples

Two lots of hydrocortisone, referred to as fine and coarse, were received from the Sigma Chemical Company (St. Louis, MO) and Upjohn Company (Kalamazoo, MI), respectively. The Upjohn sample was supplied as requested prior to micronization. Both lots were used as received.

Particle Size Analysis

Particle size analysis was performed on a Coulter counter model T_A (Coulter Electronics, Hialeah, FL). Apertures of 140 and 400 μm were used to analyze the fine and coarse lots, respectively. The suspending electrolyte, a 1% NaCl solution containing approximately 5 drops of Polysorbate 20/L, was saturated with hydrocortisone. The solution was filtered through a 0.45-μm HA-type filter (Millipore, Bedford, MA) before use.

Particle size data were assumed to be log-normally distributed. Geometric means and standard deviations were determined graphically by applying the probit transformation (11). The cumulative probability distribution $F(t)$:

$$F(t) = \frac{1}{\sqrt{2\pi}} \int_{-\infty}^{t} \exp\left[-\frac{t^2}{2}\right] \quad (1)$$

was integrated using the Runge–Kutta numerical method to determine the probits corresponding to the Coulter output. Probits were plotted versus Coulter particle size x_i plus one-half the class width d due to the grouped (11) nature of the Coulter output:

$$\text{probit} = t + 5 = \frac{\log x_i + 0.5d - \log\mu_g}{\log\sigma_g} + 5 \quad (2)$$

where μ_g is the geometric mean, σ_g is the geometric standard deviation, and $d = \log x_{i+1} - \log x_i$. A least-squares regression analysis of this plot yielded a straight line with a slope of $1/\log\sigma$ and a geometric mean corresponding to a probit of 5.

Geometric means and standard deviations were also calculated using the following equations:

$$\mu_g = \exp\left[\Sigma(\ln x_i)(f_i)\right] \quad (3)$$

$$\sigma_g = \exp\left[\Sigma(\ln x_i)^2(f_i) - (\ln\mu_g)^2\right]^{1/2} \quad (4)$$

where f_i was the fractional weight.

Simulated Distributions

Initial particle size distributions were simulated using a subroutine that divides the powder mass by using the log-normal probability density function:

$$f(r_o) = \frac{1}{\log\sigma_g\sqrt{2\pi}} \exp\left[-\frac{1}{2}\left[\frac{\log r_o - \log\mu_g}{\log\sigma_g}\right]^2\right] \quad (5)$$

Values of σ_g and μ_g were determined by the graphical regression method as described above. The upper and lower radii limits, r_{max} and r_{min}, were calculated by the following equations:

$$r_{max} = \mu_g\sigma_g^3 \quad (6)$$

[1] Central Research Division, Pfizer Inc., Groton, Connecticut 06340.

[2] To whom correspondence should be addressed.

0724-8741/93/0900-1308$07.00/0

$$r_{min} = \frac{\mu_g}{\sigma_g^3} \tag{7}$$

which can be derived from Eq. (2) by setting t equal to 3 and ignoring the 0.5 d term for grouped data. Distributions were then divided into 16 equally spaced fractions (on a logarithmic scale) and normalized to 100% to calculate the initial mass of solid drug X_{oi} corresponding to each initial particle radius r_{oi}, where the subscript i referred to the specific particle size fraction.

For simulations based on cylindrical geometry, the particle size distributions were converted from spherical radii r_s to cylindrical radii r_c through the use of a shape factor s and the assumption of equivalent volume V:

$$\frac{4}{3}\pi r_s^3 = V = \pi r_c^3 s \tag{8}$$

where $s = L/r_c$ and L is the length of the cylinder.

Simulated Dissolution

Dissolution was simulated using a previously reported method (2) based on a Noyes–Whitney-type equation (3):

$$-\frac{dX_s}{dt} = \frac{DS}{h}\left[C_s - \frac{X_d}{V}\right] \tag{9}$$

where X_s is the mass of solid drug at any time, D is the drug diffusion coefficient, S is the surface area, C_s is the solubility of the drug, h is the diffusion layer thickness, X_d is the mass of dissolved drug at any time, and V is the volume of the dissolution medium.

Simulations were performed with the surface area term of the Noyes–Whitney equation derived for spherical geometry with constant diffusion layer thickness (1,2):

$$-\frac{dX_{si}}{dt} = \frac{3DX_{oi}^{1/3}X_{si}^{2/3}}{\rho h_i r_{oi}}\left[C_s - \frac{X_d}{V}\right] \tag{10}$$

For a time-dependent diffusion layer thickness, the following relationship derived earlier (2):

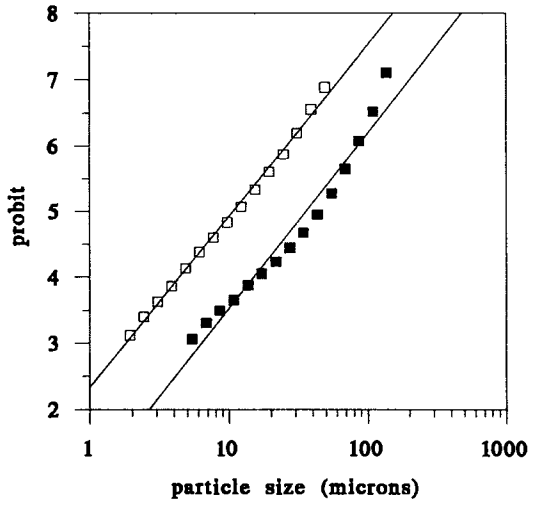

Fig. 1. Coulter counter-determined probit versus particle size of fine (open squares) and coarse (filled squares) hydrocortisone.

Table I. Geometric Means and Standard Deviations of Hydrocortisone Determined Graphically Using the Probit Transformation or Calculated Using Eqs. (3) and (4)

Lot	Method	Mean (μm)	SD
Fine	Graphical	10.7	2.4
Fine	Calculated	10.9	2.4
Coarse	Graphical	35.9	2.4
Coarse	Calculated	38.7	2.3

$$h_i = r_{oi}\left(\frac{X_{si}}{X_{oi}}\right)^{\frac{1}{3}} \tag{11}$$

was substituted into Eq. (10) to yield:

$$-\frac{dX_{si}}{dt} = \frac{3DX_{oi}^{2/3}X_{si}^{1/3}}{\rho r_{oi}^2}\left[C_s - \frac{X_d}{V}\right] \tag{12}$$

For cylindrical geometry, Eq. (9) was derived by defining the surface area term as

$$S = 2\pi r^2(1 + s)N_o \tag{13}$$

resulting in

$$-\frac{dX_{si}}{dt} = \frac{2D\,X_{oi}^{1/3}\,X_{si}^{2/3}}{\rho h_i r_{oi} s}\left[C_s - \frac{X_d}{V}\right](1 + S) \tag{14}$$

where s is the shape factor, N_o is the total number of particles, ρ is the drug density, and h_i is the diffusion layer thickness corresponding to the specific particle size fraction making up the log-normal distribution.

Substituting Eq. (11) into Eq. (14) combines a time-dependent diffusion layer thickness with cylindrical geometry:

$$-\frac{dX_{si}}{dt} = \frac{2DX_{oi}^{2/3}X_{si}^{1/3}}{\rho r_{oi}^2 s}\left[C_s - \frac{X_d}{V}\right](1 + s) \tag{15}$$

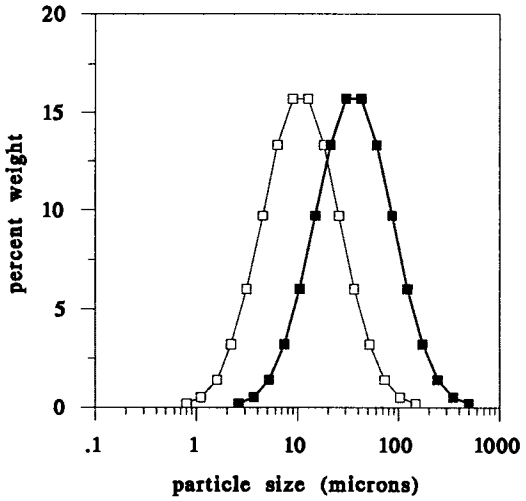

Fig. 2. Simulated log-normal particle size distributions of fine (open squares) and coarse (filled squares) hydrocortisone based on graphically determined estimates of the geometric means and standard deviations from Table 1.

Table II. Experimental Dissolution Data for Fine and Coarse Hydrocortisone

Time (min)	Percentage dissolved	
	Fine	Coarse
1	78	
2	85	
5	92	54
10	96	68
15	97	76
20	98	80.4
30	98	86.2
45	99	91
60	99	93.0

Simulations were performed by setting h_i equal to r_{oi} for particle radii less than some maximum value h_{max} and equal to this value for all greater particle radii. h_{max} was determined from the simulation with the smallest residual sum of squares. In Eqs. (12) and (15), r_{oi}^2 was replaced with $h_{max}(r_{oi})$ for particles greater than h_{max}.

Dissolution

Dissolution testing was done using an Easi-Lift Dissolution Test Station (Hanson Research Corporation, Northridge, CA) at a stirring rate of 75 rpm and a temperature of 37 ± 0.5°C; 860 mL of filtered and degassed deionized water was placed in the vessel and heated. The USP paddle method was followed.

About 150 mg of hydrocortisone powder was accurately weighed into a clean glass vial along with 15 mg of sodium lauryl sulfate (added as a wetting agent). The powder was

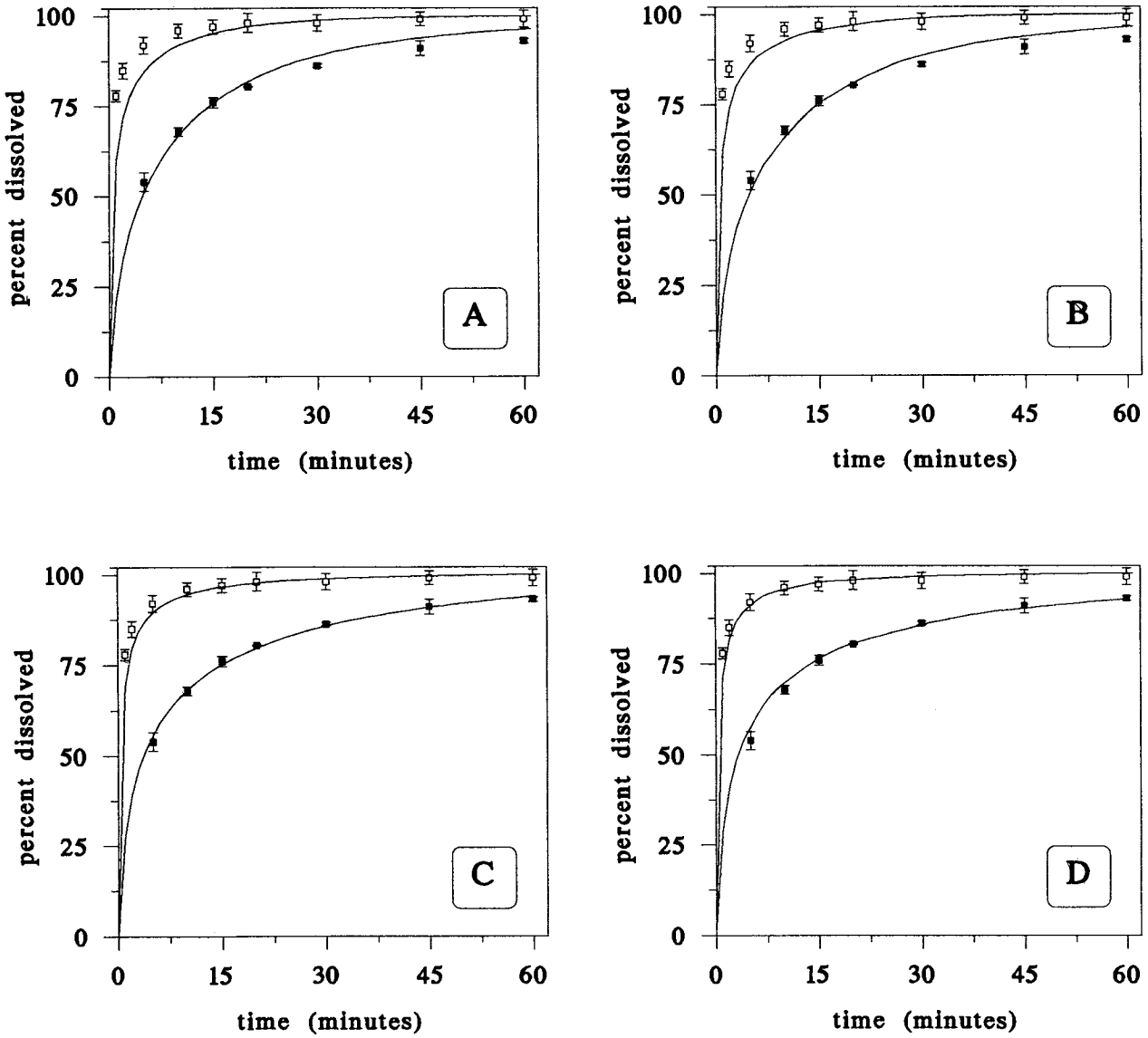

Fig. 3. Dissolution profiles of fine (open squares) and coarse (filled squares) hydrocortisone. Simulated curves were drawn using spherical geometry without (A) and with (B) a time-dependent diffusion layer thickness and cylindrical geometry without (C) and with (D) a time-dependent diffusion layer thickness. Error bars represent 95% CI (n = 3).

Table III. Residual Values from Simulations in Fig. 3

	Spherical geometry time-independent h, h_{max} = 14		Spherical geometry time-dependent h, h_{max} = 18		Cylindrical geometry time-independent h, h_{max} = 22		Cylindrical geometry time-dependent h, h_{max} = 32	
Time	Fine	Coarse	Fine	Coarse	Fine	Coarse	Fine	Coarse
1	329		239		79		41	
2	181		125		33		12	
5	57	8	34	9	7	3	1	13
10	17	1	12	4	2	0	0	3
15	4	0	2	0	0	1	0	0
20	1	2	1	0	0	0	0	0
30	1	7	1	6	1	0	1	0
45	0	8	1	8	0	0	0	1
60	1	10	1	12	1	1	1	0
Sum of squares	591	36	416	39	123	5	56	17

prewetted with mild sonication, the suspension was poured quickly into the dissolution vessel, and the vial was rinsed using a total of 40 mL of water.

Sample Assay

At specified time intervals, 5-mL samples were removed by pipet and filtered through 0.22-μm Millex GS filter units (Millipore), discarding the first 2–3 mL. The filtered solutions were then diluted 1:10 with HPLC-grade methanol and immediately assayed on a Lambda 3B UV/Vis Spectrophotometer (Perkin Elmer, Norwalk, CT) at a wavelength of 242 nm.

SEM Micrographs

Scanning electron micrographs were taken on a JSM-840 Scanning Microscope (JEOL, Peabody, MA). Estimates of shape factor were made directly from these micrographs using a millimeter ruler. Several representative particles were measured to determine the average length to width ratios.

Modeling Parameters

Other physical parameters used in modeling were determined as follows. The saturation solubility of hydrocortisone in dissolution media with sodium lauryl sulfate was found by adding an excess of drug to about 10 mL in a clean vial with a screw cap. The vial was placed in a water bath set at 37 ± 0.5°C and rotated end over end for 72 hr. After removal, the sample was quickly filtered and diluted before assay. Solubility was found to be 0.361 mg/mL.

A diffusion coefficient of 3.52×10^{-4} cm^2/min was used based on an estimate of the molecular volume of hydrocortisone and the Hayduk–Laudie correlation (12). The true density of hydrocortisone was measured to be 1270 ± 20 mg/cm^3 (95% CI) using a micropycnometer (Quantachrom, Syosset, NY).

RESULTS

The Coulter counter cumulative fractional weight particle size data was converted to probits and plotted versus particle size as shown in Fig. 1. Least-squares linear regression analyses were performed which resulted in residual values of 0.073 and 0.799 for the fine and coarse samples, respectively. Although there is a larger systematic deviation from pure log-normal behavior for the coarse hydrocortisone, we considered the approximation to be reasonable for our simulation purposes. The geometric mean diameters and standard deviations were determined from these best-fit lines. For comparison, these values were also calculated using Eqs. (3) and (4). The results are summarized in Table I. Both methods gave similar results, however, the graphical regression results were used for the simulations presented in this paper.

Figure 2 shows the simulated log-normal particle size distributions based on σ_g and μ_g values determined by the graphical method. The percentage weight values were used to calculate X_{oi} in Eqs. (10), (12), (14), and (15).

Table II shows the experimental dissolution data of the two lots of hydrocortisone. The computer model was used to simulate this data based on spherical and cylindrical geometry, with and without a time-dependent diffusion layer as shown in Fig. 3. Table III shows the h_{max} and least-squares residuals used for each simulation. A shape factor of 4 was used for the cylindrical geometry simulations and was estimated from the scanning electron micrographs shown in Fig. 4.

DISCUSSION

Solubility, surface area, and hydrodynamics are three important factors affecting the dissolution rate of polydisperse powders. While solubility and surface area can be determined in a straightforward manner, no clear-cut method exists for determining the hydrodynamic diffusion layer thickness. Higuchi and Hiestand (4) suggested that h is comparable to the particle radius, but Harriott's work (13) demonstrated that this trend would not continue for larger particles and that h would reach a plateau. These observations were combined in previous simulations (2) by setting h equal to the particle radius for small particles (particle radius <30 μm) and equal to 30 μm for all larger particles. Recently, the general validity of this treatment has been confirmed inde-

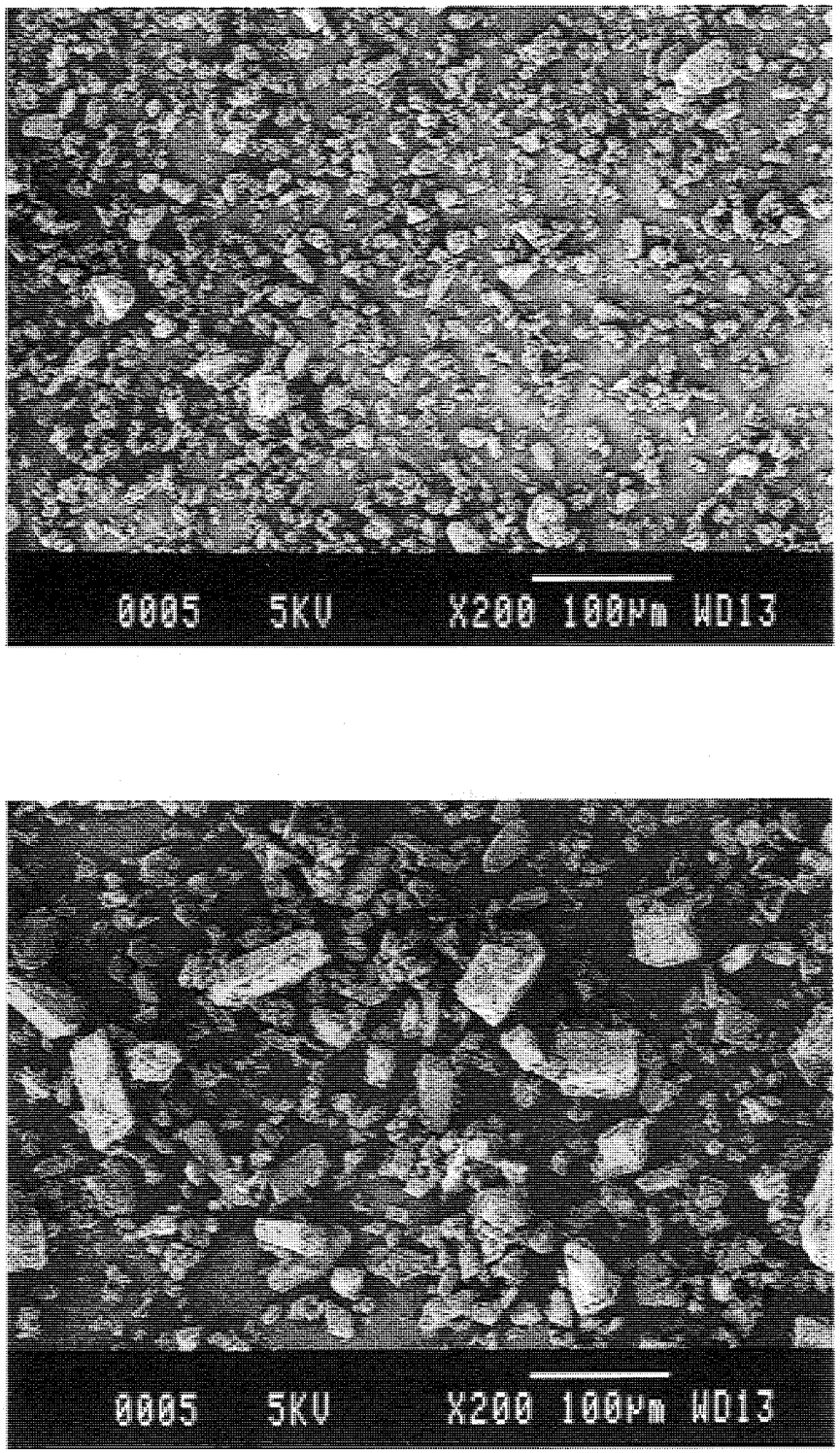

Fig. 4. Scanning electron micrographs of fine and coarse hydrocortisone.

pendently (14). We prefer this method because of its simplicity and the accuracy of the simulations obtained.

The prior selection of 30 μm as h_{max} was based on results from intrinsic dissolution studies using a rotating disk and was not rigorously applicable to the dissolution of suspended particles. In the simulations shown in Fig. 3, an unbiased value of h_{max} was determined from the least-squares simulation of the coarse dissolution data for each of the four theoretical dissolution equations. The coarse data were used to determine h_{max} because we had greater confidence in the accuracy of the data determined from the slower-dissolving hydrocortisone. This is because the rate of dissolution for the fine material was fast relative to the sampling time at early time points. Also, a greater amount of dissolution may

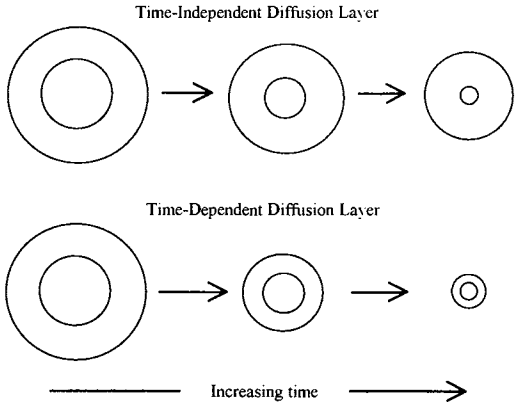

Fig. 5. Schematic representation of time-independent versus time-dependent diffusion layer thickness for spherical particles.

have occurred during the prewetting stage for the fine hydrocortisone relative to the coarse. This would explain why using the same h_{max} underestimated the dissolution rate of fine hydrocortisone.

The potential inaccuracy in assuming a time-independent diffusion layer thickness has been criticized (2,15). Since the diffusion layer is generally believed to be comparable to the particle radius (4), the diffusion layer should decrease as a particle decreases in size during dissolution. If the diffusion layer is kept at its initial value, it becomes increasingly more unrealistic as the particle becomes smaller. Figure 5 shows this concept in schematic form. We were interested in seeing what effect incorporating a time-dependent diffusion layer thickness might have on the accuracy of the simulations. Simulations of the coarse dissolution data using a time-dependent h resulted in a slight decrease in accuracy for both spherical and cylindrical geometries. For the fine dissolution simulations, a greater improvement was seen in both cases.

Although the Coulter counter can measure the volume of nonspherical particles (16–18), it reports the particle sizes based on volume-equivalent spheres (19). Because dissolution rate is dependent on surface area according to Eq. (9), and a sphere has the smallest surface area/volume ratio of any geometry, simulated dissolution rates of nonspherical particles based on uncorrected Coulter particle sizes will be slower than actual. We have chosen to use a cylindrical geometry with a shape factor to make this correction. Cylindrical geometry has the potential of describing particle shapes ranging from plates to needles by changing the shape factor (Fig. 6). For both fine and coarse dissolution simulations, surface area corrections using cylindrical geometry resulted in an improvement in accuracy.

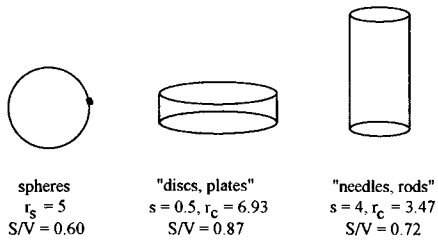

Fig. 6. Comparison of surface area-to-volume ratios for spherical and cylindrical geometries with equivalent volumes and indicated shape factors.

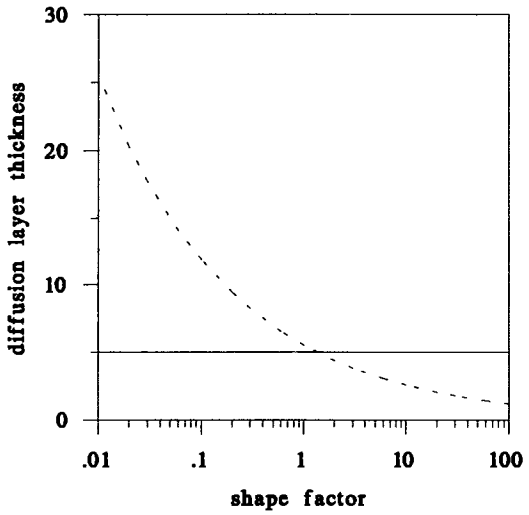

Fig. 7. Diffusion layer thickness versus shape factor for a sphere (solid line) and cylinder (dashed line) with equivalent volumes.

For both cylindrical and spherical geometry, h was set equal to the radius for particle radii less than h_{max}. However, for a shape factor of 4, the cylindrical radius is smaller than the volume equivalent spherical radius, and therefore, h is also smaller as shown in Fig. 7. As a result, the accuracy of simulations using cylindrical geometry is affected by a decrease in h as well as an increase in surface area as shown in Fig. 8. Although our treatment of nonspherical particles through the use of cylindrical geometry and a shape factor improved the accuracy of dissolution simulations, we would not recommend the analysis for shape factors deviating greatly from 2, where surface area is a minimum. This is due to the uncertainty of modeling h for grossly nonspherical particles.

There are other potential pitfalls when using a cylindrical geometry. Particles with nonspherical geometries may

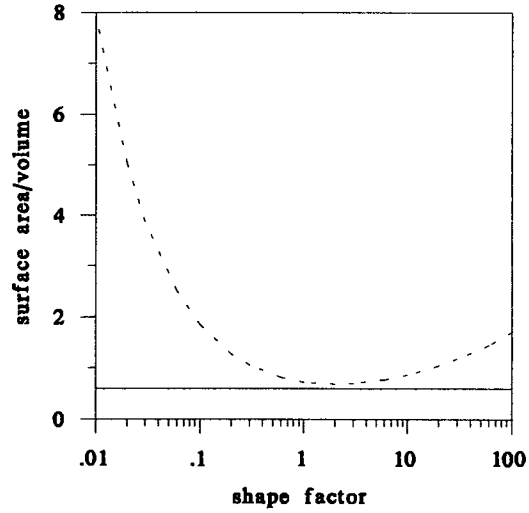

Fig. 8. Surface area-to-volume ratio versus shape factor for a sphere (solid line) and cylinder (dashed line) with equivalent volumes.

not have a uniform diffusion layer thickness over the entire surface. This being the case, dissolution may occur at different rates from the various faces leading to a change in particle shape over time. A more rigorous model may take into account the time dependency of particle shape. However, the benefits of using a cylindrical geometry to mimic the shape of the hydrocortisone particles are clear. By allowing more accurate estimations of particle surface area, the shape of the simulated dissolution profiles is improved, leading to the best fit of the experimental data.

Previous simulations (2) made no assumptions about the functional form of particle size distributions. This made it necessary to report the exact percentage weight of powder in each particle size fraction to specify the conditions of simulated dissolution profiles. Changes in the total powder mass or shifts in the weight distributions required tedious calculations. To overcome this problem, the log-normal probability density function was used to generate initial particle size distributions. This function has been widely used to characterize particulate systems (4–10). However, not all powders can be adequately described by this function, and a graphical analysis of particle size data will help identify those powders.

The dissolution rates of two lots of hydrocortisone were simulated to demonstrate that the model has adequate sensitivity to changes in particle size distributions. Model improvements were also considered separately to demonstrate the magnitude of each improvement on simulated dissolution, although a combination of assumptions may be closer to reality.

In summary, using a more realistic geometry to calculate surface area improved the accuracy of dissolution simulations for both fine and coarse hydrocortisone. Although a time-dependent h may seem intuitively more realistic, simulations of the data did not clearly support this. More work needs to be done to determine if a time-dependent diffusion layer thickness would generally lead to more accurate simulations.

ACKNOWLEDGMENTS

We would like to thank Mr. Richard I. Boyd, Dr. David S. Salsburg, and Dr. Archie C. Swindell for their assistance.

REFERENCES

1. J. B. Dressman and D. Fleisher. Mixing-tank model for predicting dissolution rate control of oral absorption. *J. Pharm. Sci.* 75:109–116 (1986).
2. R. J. Hintz and K. C. Johnson. The effect of particle size distribution on dissolution rate and oral absorption. *Int. J. Pharm.* 51:9–17 (1989).
3. A. A. Noyes and W. R. Whitney. The rate of solution of solid substances in their own solutions. *J. Am. Chem. Soc.* 19:930–934 (1897).
4. W. I. Higuchi and E. N. Hiestand. Dissolution rates of finely divided drug powders I. Effect of a distribution of particle sizes in a diffusion-controlled process. *J. Pharm. Sci.* 52:67–71 (1963).
5. S. E. LeBlanc and H. S. Fogler. Population balance modeling of the dissolution of polydisperse solids: Rate limiting regimes. *AIChE J.* 33:54–63 (1987).
6. T. Allen. *Particle Size Measurement,* 3rd ed., Chapman and Hall, New York, 1981.
7. J. D. Stockham and E. G. Fochtman. *Particle Size Analysis,* Ann Arbor Science, Ann Arbor, MI, 1978.
8. J. T. Carstensen and M. N. Musa. Dissolution rate patterns of log normally distributed powders. *J. Pharm. Sci.* 61:223–227 (1972).
9. D. Brooke. Dissolution profile of log-normal powders: Exact expression. *J. Pharm. Sci.* 62:795–798 (1973).
10. Y. Yonezawa, I. Shinohara, A. Otsuka, and H. Sunada. Changes of surface area in the dissolution process of crystalline substances. V. Dissolution and simulation curves for log-normal particle-size distributed model systems. *Chem. Pharm. Bull.* 38:1024–1026 (1990).
11. K. Diem and C. Lenter. *Scientific Tables,* GEIGY Pharmaceuticals, New York, 1970.
12. R. C. Reid, J. M. Prausnitz, and T. K. Sherwood. *The Properties of Gases and Liquids,* McGraw–Hill, New York, 1977.
13. P. Harriott. Mass transfer to particles. I. Suspended in agitated tanks. *AIChE J* 8:93–101 (1962).
14. M. Bisrat, E. K. Anderberg, M. I. Barnett, and C. Nyström. Physicochemical aspects of drug release. XV. Investigation of diffusional transport in dissolution of suspended, sparingly soluble drugs. *Int. J. Pharm.* 80:191–201 (1992).
15. J. Mauger and S. Howard. Model systems for dissolution of finely divided (multisized) drug powders. *J. Pharm. Sci.* 65:1042–1045 (1976).
16. H. N. Rosen and H. M. Hulbert. Size analysis of irregular shaped particles in sieving. Comparison with the Coulter counter. *Ind. Eng. Chem. Fund.* 9:658–661 (1970).
17. P. J. Lloyd. Response of the electrical sensing zone method to nonspherical particles. In N. G. Stanley-Wood and T. Allen (eds.), *Particle Size Analysis 1981,* Wiley Heyden Ltd., London, 1981.
18. R. K. Eckhoff. Experimental indication of the volume proportional response of the Coulter counter for irregularly shaped particles. *J. Sci. Instrum.* 44:648–649 (1967).
19. Coulter Electronics. *Coulter Counter Model TA Instruction and Service Manual,* Hialeah, FL, 1972.